

Elsevier Editorial System(tm) for Fish and Shellfish Immunology

Manuscript Draft

Manuscript Number: FSIM-D-07-00013R1

Title: MOLECULAR CLONING, DIFFERENTIAL EXPRESSION AND 3D STRUCTURAL ANALYSIS OF THE MHC CLASS-II beta CHAIN FROM SEA BASS (*Dicentrarchus labrax* L.)

Article Type: Full Length Article

Section/Category:

Keywords: major histocompatibility complex class (MHC) II beta chain; sea bass; *Dicentrarchus labrax*; cloning; polymorphism; expression analysis; quantitative PCR; 3D structure.

Corresponding Author: Dr Francesco Buonocore, PhD

Corresponding Author's Institution: University of Tuscia

First Author: Francesco Buonocore, PhD

Order of Authors: Francesco Buonocore, PhD; Elisa Randelli, PhD; Daniela Casani, PhD student; Susan Costantini; Angelo Facchiano, PhD; Giuseppe Scapigliati, PhD; Renè J Stet

Manuscript Region of Origin:

Abstract: The major histocompatibility complex class I and II molecules (MHC-I and MHC-II) plays a pivotal role in vertebrate immune response to antigenic peptides. In this paper we report the cloning and sequencing of the MHC class II b chain from sea bass (*Dicentrarchus labrax* L.). The six obtained cDNA sequences (designated as Dila-DAB) code for 250 amino acids, with a predicted 21 amino acid signal peptide and contain a 28 bp 5'-UTR and a 478 bp 3'-UTR. A multiple alignment of the predicted translation of the Dila-DAB sequences was assembled together with other fish and mammalian sequences and it showed the conservation of most amino acid residues characteristic of the MHC class II b chain structure. The highest basal Dila-DAB expression was found in gills, followed by gut and thymus, lower mRNA levels

were evidenced in spleen, peripheral blood leucocytes (PBL) and liver. Stimulation of head kidney leucocytes with LPS for 4 h showed very little difference in the Dila-DAB expression, but after 24 h the Dila-DAB level decreased to a large extent and the difference was statistically significant. Stimulation of head kidney leucocytes with different concentrations of rIL-1b (ranging from 0 to 100 ng/ml) resulted in a dose-dependent reduction of the Dila-DAB expression. Moreover, two 3D Dila-DAB\*0101 homology models were obtained based on crystallographic mouse MHC-II structures complexed with D10 T-cell antigen receptor or human CD4: features and differences between the models were evaluated and discussed. Taken together these results are of interest as MHC-II structure and function, molecular polymorphism and differential gene expression are in correlation with disease resistance to virus and bacteria in teleost fish.

Dear Prof. Tony Ellis,

I am sending you a revised version of the paper entitled: "MOLECULAR CLONING, DIFFERENTIAL EXPRESSION AND 3D STRUCTURAL ANALYSIS OF THE MHC CLASS-II beta CHAIN FROM SEA BASS (*Dicentrarchus labrax* L.)" (Ref. n. FSIM-D-07-00013), author team: Francesco Buonocore, Elisa Randelli, Daniela Casani, Susan Costantini, Angelo Facchiano, Giuseppe Scapigliati, Renè J.M. Stet.

I have taken into account most of the suggestions from the referees and I have attached a list of all the changes made in the paper (in the text you will find **in bold** the phrases that differ from the first version).

I hope that now the paper will be accepted for the publication, but let me know if there is any problem.

Best regards

Dr. Francesco Buonocore

Dear Prof. Tony Ellis,

I am sending you a revised version of the paper entitled: "MOLECULAR CLONING, DIFFERENTIAL EXPRESSION AND 3D STRUCTURAL ANALYSIS OF THE MHC CLASS-II beta CHAIN FROM SEA BASS (*Dicentrarchus labrax* L.)" (Ref. n. FSIM-D-07-00013), author team: Francesco Buonocore, Elisa Randelli, Daniela Casani, Susan Costantini, Angelo Facchiano, Giuseppe Scapigliati, Renè J.M. Stet.

I have taken into account most of the suggestions from the referees and I have attached a list of all the changes made in the paper (in the text you will find **in bold** the phrases that differ from the first version).

I hope that now the paper will be accepted for the publication, but let me know if there is any problem.

Best regards

Dr. Francesco Buonocore

#### **Reviewer #1:**

This manuscript describes the cloning of 6 cDNA sequences encoding MHC class II beta from sea bass. The sequences have been aligned and analyzed in a phylogenetic tree, the expression of the gene in head kidney leukocytes in response to stimulation with LPS and II-beta is examined by real time PCR and some homology models have been derived.

#### **General Comments**

This paper is generally well written, although the English need polishing. The data provided are interesting, but much of it is in silico derived from the sequences and the addition of a few more "wet lab" experiments would greatly enhance the story the authors are trying to tell. For example, sequencing cDNAs does not really give gene copy number or even number of expressed genes due to primer bias/fit among other problems. The addition of a Southern blot, an analysis of the expression levels in different tissues or the examination of the real degree of polymorphism by sequencing the putative PBR regions from several other individuals (up to 50 sequences) would provide more evidence that these are the functional genes of Sea Bass and enhance the publish ability of this manuscript.

**I have added an analysis of the MHC expression levels in different tissues. The Southern blot has not been added as an attempt to evidence the number of class II B loci in sea bass is already present in the paper (see the beginning of "Results" section). The examination of the real degree of polymorphism was not in the aim of the authors, but the idea was to focus on the analysis of functional evidences related to the MHC gene.**

The discussion is very weak and fails to discuss important questions such as why the expression of genes that are key to the immune response is down-regulated after stimulation - this seems to mean that the immune response is being shut down. The rest of the discussion needs more explanation of the data rather than simply saying it agrees or disagrees with the literature.

**I have improved the Discussion taking into account the reviewer suggestions.**

**Specific comments:**

line 63: Redundant language

**I have changed the phrase.**

line 65: in terms of linkage? Polymorphism? Classical/non-classical? Clarify

**I have clarified the sentence.**

line 229 "they encode"

**I have corrected the mistake.**

line 244; 11% identity - no "of"

**I have corrected the mistake.**

line 257 ; The trout glycosylation site is more than just "potential" the protein is definitely glycosylated - see: Immunogenetics (2006) 58: 443-453

**“Potential” was referred to sea bass and not to the other species, I have added the reference.**

Line 258: Figure 2 - why were amino acid sequences used? DNA has more usable data and avoid convergence more. Why are some names capitalized and others not?

**Yes, usually DNA has more usable data and avoid convergence more, but we got similar results with DNA or amino acid, so we decide to use the latter as it was more straightforward after the alignment. I have used only capitalized names in the tree.**

Line 265, figure 3 Did you measure IL-1b expression after LPS stimulation to ensure you actually got stimulation? (oh I see you did at line 392-394 - you should mention this earlier). Sometimes LPS doesn't work so well on fish, especially from E coli. This concentration seems very low - other papers have used as much as 100ug/ml. Why was this concentration chosen - was a preliminary experiment using a range of concentrations done to assess how much is needed to elicit a response? Why did the expt only go to 24 hours? It seems that MHC expression should be affected for a long time after that.

**I have added a phrase in the “Results” section related to the studying of IL-1 $\beta$  expression to ensure LPS stimulation. The LPS concentration worked well in a lot of different experiments we performed in the past (for a reference see: G. Scapigliati, F. Buonocore, S. Bird, J. Zou, P. Pelegrin, C. Falasca, D. Prugnoli and C.J. Secombes. Phylogeny of cytokines: molecular cloning and expression analysis of sea bass *Dicentrarchus labrax* interleukin-1 $\beta$ . *Fish and Shellfish Immunology* (2001), 11(8):711-726; F. Buonocore, E. Randelli, D. Casani, M. Mazzini, I. Cappuccio, C.J. Secombes, G. Scapigliati. cDNA cloning and expression analysis of a cyclooxygenase-2 from sea bass (*Dicentrarchus labrax* L.) after vaccination. *Aquaculture* (2005), 245(1-4): 301-310; F. Buonocore, M. Forlenza, E. Randelli, S. Benedetti, P. Bossù, S. Meloni, C.J. Secombes, M. Mazzini, G. Scapigliati. Biological activity of sea bass (*Dicentrarchus labrax*) recombinant interleukin-1 $\beta$ . *Marine Biotechnology* (2005), 7(6): 609-617), so we used the same. We did not look at the MHC expression after 24 h both because LPS elicit inflammatory responses quickly (few hours post-stimulation) and as the viability of**

fish leukocyte cultured cells is quite low, so to study the MHC expression for a long time we should perform “in vivo” experiments.

Line 290 is 34% identity enough to do this?

Yes, it is enough with the used computational methods (for a reference see: Facchiano AM, Stiuso P, Chiusano ML, Caraglia M, Giuberti G, Marra M, et al. Homology modelling of the human eukaryotic initiation factor 5A (eIF-5A). *Protein Engineering* 2001; 14: 881-90; Marabotti A, D’Auria S, Rossi M, Facchiano AM. Theoretical model of the three-dimensional structure of a sugar binding protein from *Pyrococcus horikoshii*: structural analysis and sugar binding simulations. *Biochem J* 2004; 280:677-84). I have added a phrase in the “Results” section.

Line 369-370: there is variability - you can't say it is "high" based on 6 sequences

**I have changed the phrase.**

Lines 393-403: but why does MHC expression go down - this is decreasing the immune response in response to a simulated infection - isn't this bad?? You need to discuss the implications of this? Does the MHC expression increase later????

**MHC down-regulation in our samples could be very likely linked to the already reported mechanisms for the control of inflammation responses in mammals that, uncontrolled, may have dangerous effects. For example, during early inflammation, various cytokines are produced and they down-regulate the expression of inflammation-related molecules.**

**Reviewer #2**

**General comments:**

The manuscript outlines the isolation and structural analysis of six full length MHC class II B sequences cDNA sequences in Sea Bass, a topic which should be of relevance and interest to the readership of *Fish and Shellfish Immunology*. While I can't speak authoritatively about the structural analysis, the science appears sound and the methods clear. There are a few instances where the English wording could use improvement (see below), but generally the manuscript is well organised and written.

I would have liked further elaboration about the potential impact of the modeling exercise on our understanding of the function of this gene.

**I have improved the Discussion taking into account the reviewer suggestions.**

Given that the two models differed in perhaps the most important site-the ligand binding region, how can one differentiate which is correct?

**The two models represent two conformations of the same protein under different conditions, i.e. the interaction with two different ligands, and this may explain why the main structural differences involve the binding sites, as observed by the referee. It is not possible to indicate if one model is better than the other. Each model predicts the structural organization of the protein when it interacts with CD4 or TCR, so both models can be useful for further experimental studies to simulate the interaction with the respective ligand and confirm the structural prediction.**

How does the size of the binding site relate to the size of the potential ligand?

**The binding sites for the antigen peptide and CD4 resulted larger in the MHC conformation which interacts with these ligands, and the binding site for TCR resulted larger in the MHC conformation which interacts with TCR. We wrote that this observation confirms the reliability of the two models. In fact, this results is in agreement with the ability of any protein to adopt a conformation more suitable to the interaction. The larger surface implies a better ability to interact with the ligand. As an example, it is well known that enzymes expose better the catalytic site in the presence of the substrate. Therefore, the measures of the surfaces for the binding sites confirm that our models are suitable to simulate the different conformations of MHC when it interacts with the two different ligands.**

The authors should consider revising their final concluding sentence, as it is too long and cumbersome. As a note, they have not demonstrated that the genes they identified are actually maintained by pathogen-driven selection.

**The final sentence has been revised.**

**English could be better in places, some of which are outlined below:**

Line 194: significativity -- what is that? Should be significance

**I have changed the word.**

Line 232: in order to verify the number of class II B locus (should be loci)

**I have changed the word.**

Line 233: perfomed should be performed

**I have changed the word.**

Line 239: seems to express up to three class II b loci at least (up to and at least are contradictory terms. Should read at least three class IIb loci)

**I have changed the phrase.**

Line 325: where the strands include less amino acids (should read fewer amino acids)

**I have changed the word.**

Line 361: growing evidences suggest should read growing evidence suggests

**I have changed the phrase.**

Line 397: I am not sure what is meant by similar results...after infection with IHNV on MHC class I-what? That expression of class I or class II was downregulated?

**I have changed the phrase.**

Line 404: the identity percentage should read percentage identity

**I have changed the phrase.**



Figure 2

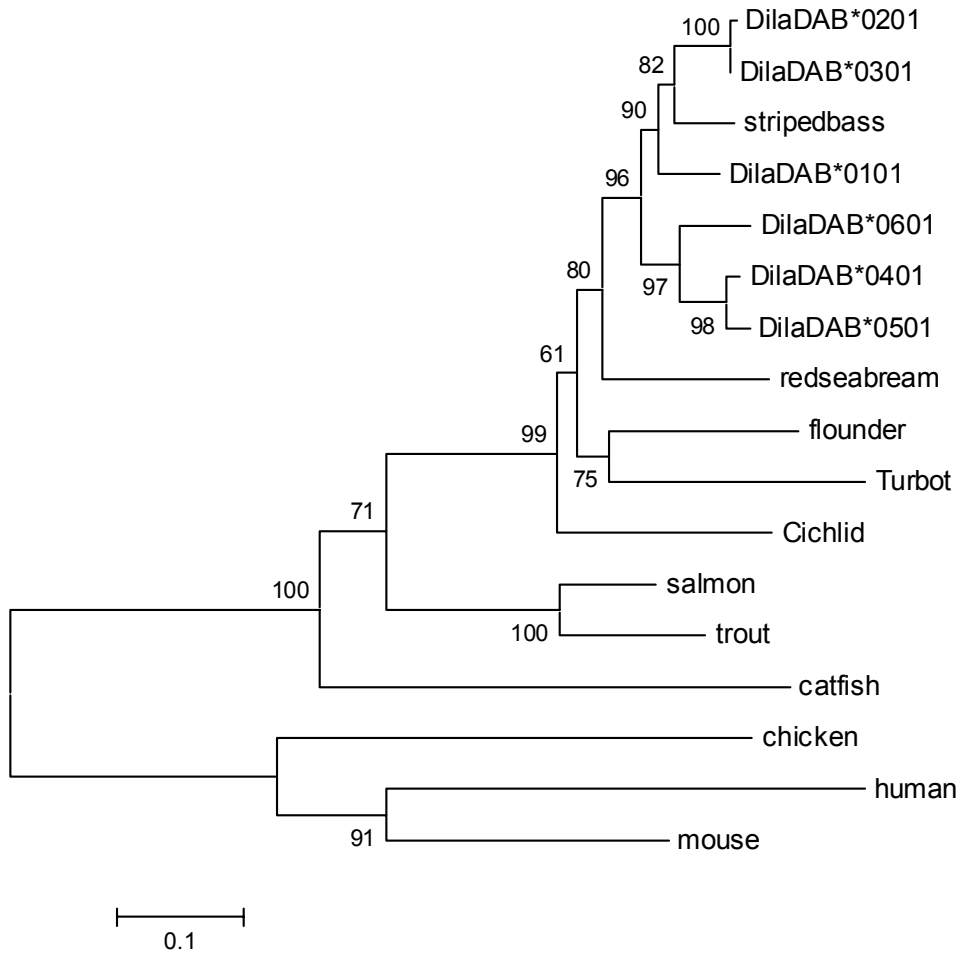
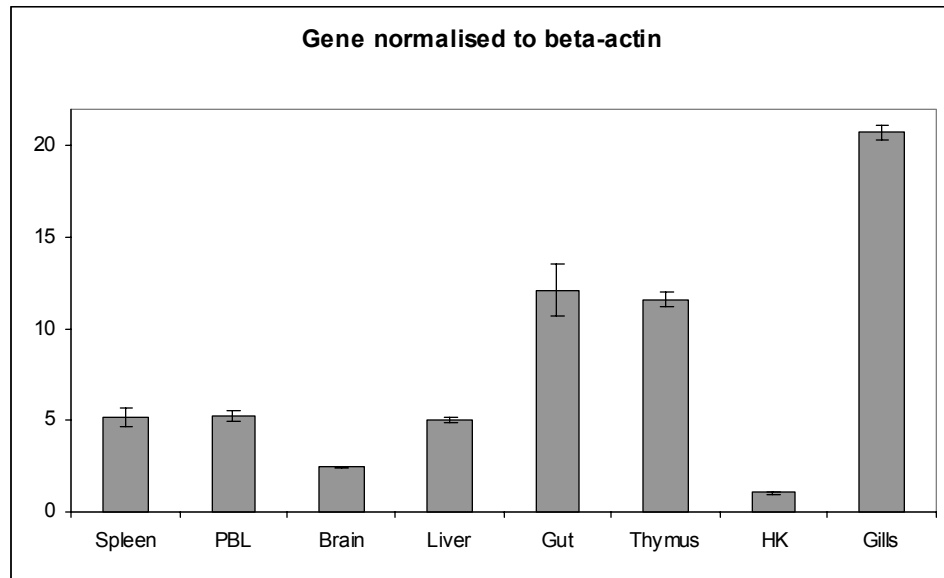


Figure 3



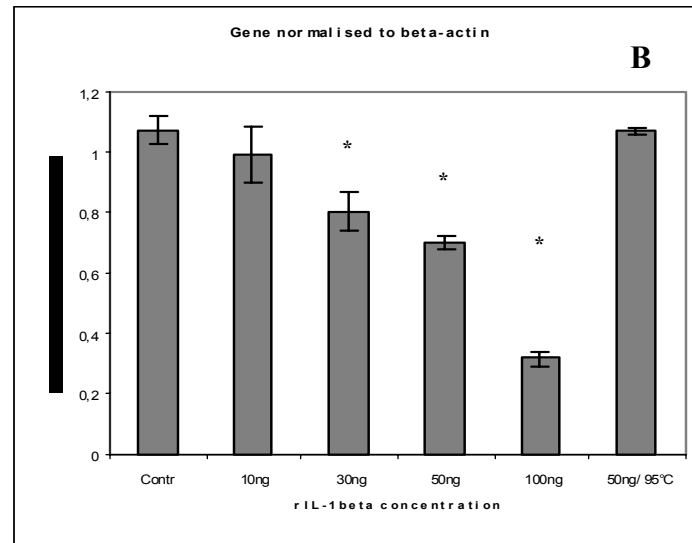
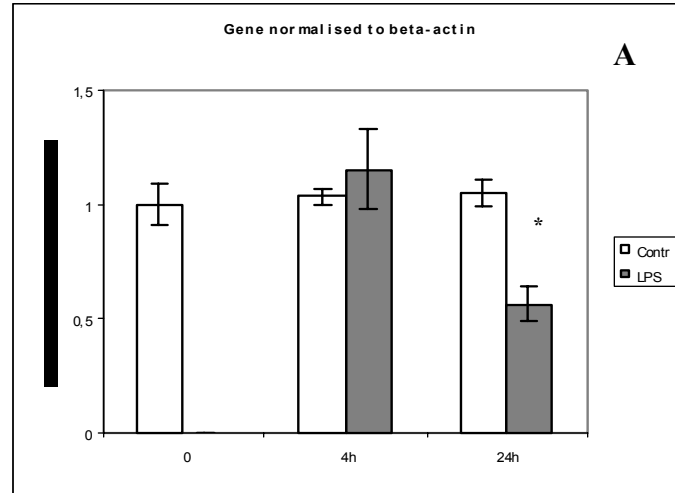


Figure 5

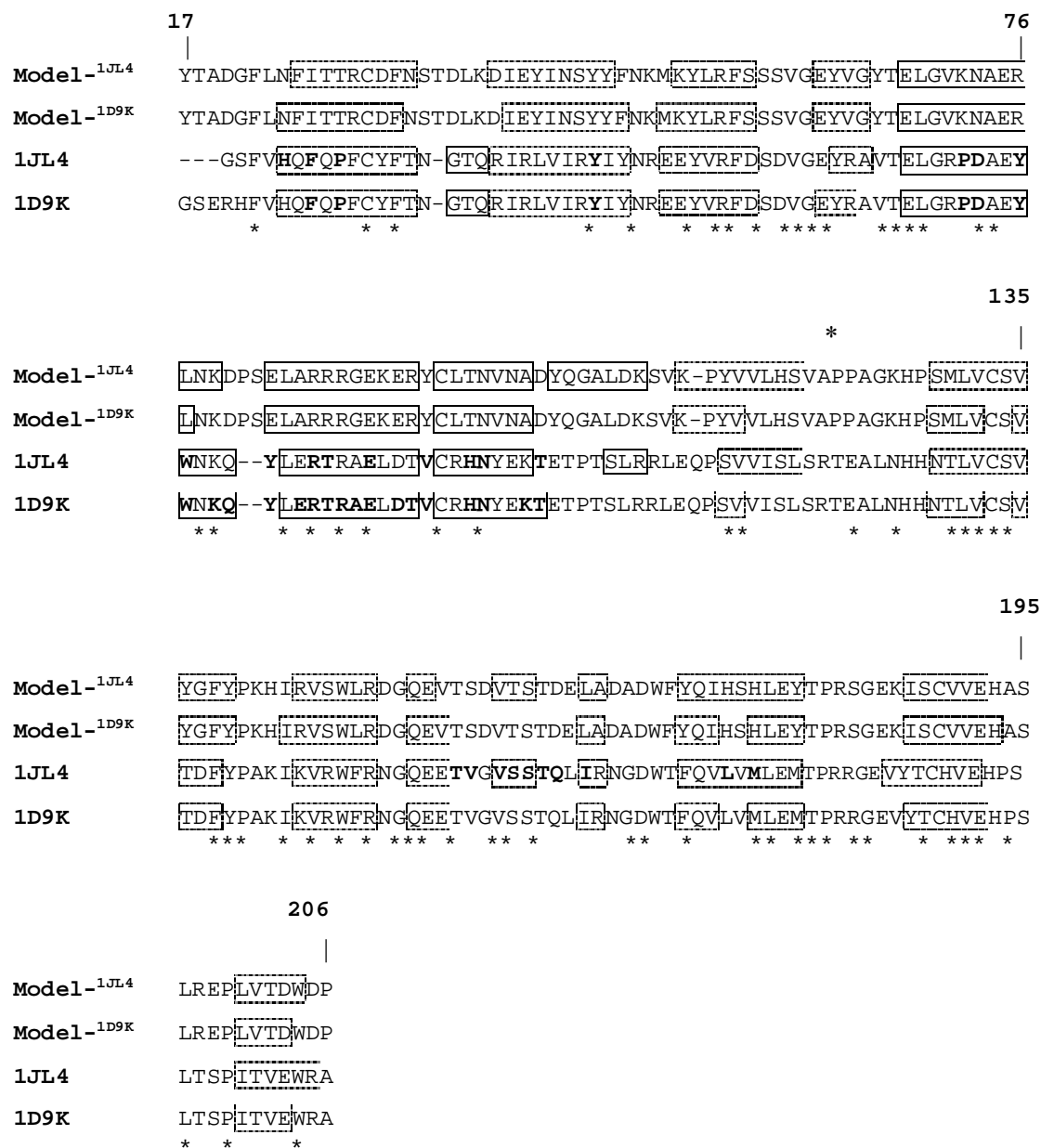
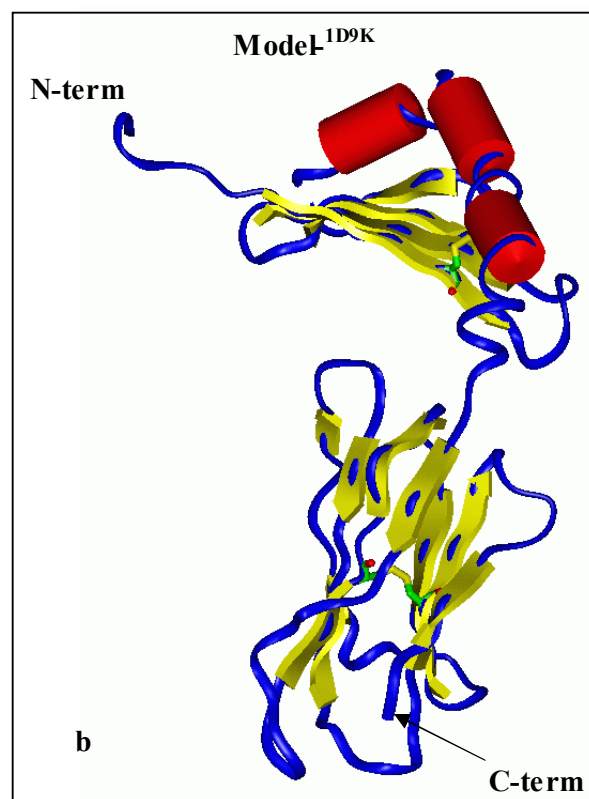
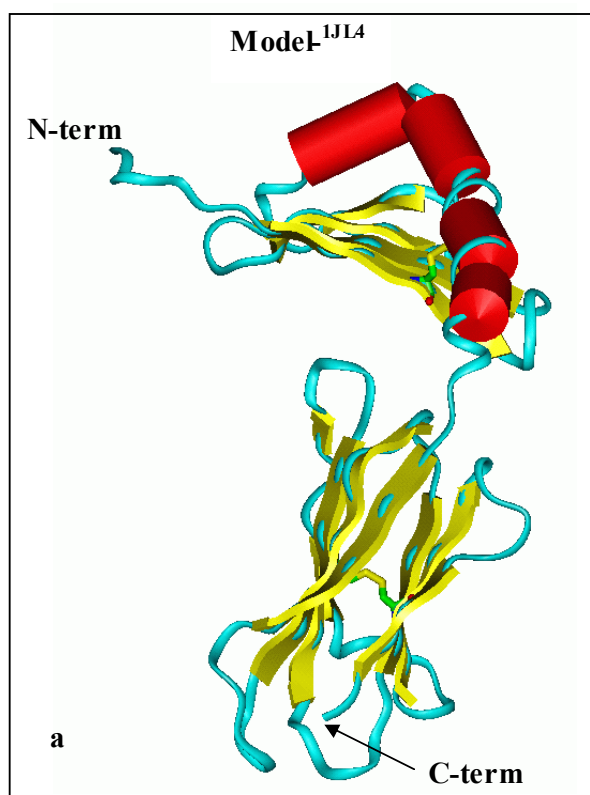


Figure 6



1  
2 **MOLECULAR CLONING, DIFFERENTIAL EXPRESSION AND 3D**  
3 **STRUCTURAL ANALYSIS OF THE MHC CLASS-II  $\beta$  CHAIN FROM SEA**  
4 **BASS (*Dicentrarchus labrax* L.)**

5  
6 **Francesco Buonocore\***, **Elisa Randelli**, **Daniela Casani**, **Susan Costantini**<sup>2</sup>,  
7 **Angelo Facchiano**<sup>2</sup>, **Giuseppe Scapigliati**, **Renè J.M. Stet**<sup>1</sup>

8 Dipartimento di Scienze Ambientali, University of Tuscia, Largo dell'Università, 01100 Viterbo,  
9 Italy

10 <sup>1</sup>Scottish Fish Immunology Research Centre, University of Aberdeen, Tillydrone Avenue, AB24  
11 2TZ Aberdeen, Scotland, UK.

12 <sup>2</sup>CNR, Istituto di Scienze dell'Alimentazione, I-83100 Avellino, Italy

13  
14  
15 **\*Corresponding author:** Dr. Francesco Buonocore, Dipartimento di Scienze Ambientali,  
16 Università della Tuscia, Largo dell'Università s.n.c., I-01100 Viterbo, Italy.

17 Phone +39-0761-357644; Fax +39-0761-357179; Email: fbuono@unitus.it

## ABSTRACT

The major histocompatibility complex class I and II molecules (MHC-I and MHC-II) plays a pivotal role in vertebrate immune response to antigenic peptides. In this paper we report the cloning and sequencing of the MHC class II  $\beta$  chain from sea bass (*Dicentrarchus labrax* L.). The six obtained cDNA sequences (designated as Dila-DAB) code for 250 amino acids, with a predicted 21 amino acid signal peptide and contain a 28 bp 5'-UTR and a 478 bp 3'-UTR. A multiple alignment of the predicted translation of the Dila-DAB sequences was assembled together with other fish and mammalian sequences and it showed the conservation of most amino acid residues characteristic of the MHC class II  $\beta$  chain structure. **The highest basal Dila-DAB expression was found in gills, followed by gut and thymus, lower mRNA levels were found in spleen, peripheral blood leucocytes (PBL) and liver.** Stimulation of head kidney leukocytes with LPS for 4 h showed very little difference in the Dila-DAB expression, but after 24 h the Dila-DAB level decreased to a large extent and the difference was statistically significant. Stimulation of head kidney leukocytes with different concentrations of rIL-1 $\beta$  (ranging from 0 to 100 ng/ml) resulted in a dose-dependent reduction of the Dila-DAB expression. Moreover, two 3D Dila-DAB\*0101 homology models were obtained based on crystallographic mouse MHC-II structures complexed with D10 T-cell antigen receptor or human CD4: features and differences between the models were evaluated and discussed. Taken together these results are of interest as MHC-II structure and function, molecular polymorphism and differential gene expression are in correlation with disease resistance to virus and bacteria in teleost fish.

**Keywords:** major histocompatibility complex class (MHC) II  $\beta$  chain; sea bass; *Dicentrarchus labrax*; cloning; polymorphism; expression analysis; quantitative PCR; 3D structure.

## 1. INTRODUCTION

49

50 The major histocompatibility complex class I and II molecules (MHC-I and MHC-II) are  
51 fundamental components of the immune response to foreign protein antigens. They have been  
52 extensively studied in mammals, especially in humans [1], mouse and rat. The MHC molecules are  
53 heterodimers formed by  $\alpha$  and  $\beta$  membrane glycoproteins that bind self and non-self peptides for  
54 presentation on the cell surface to T-cells. MHC-II binds peptides for presentation to the CD4<sup>+</sup> T  
55 helper cells [2-3] and it is encoded by two genes, *A* and *B* [4], in mammals. MHC-II genes are  
56 constitutively expressed in antigen-presenting cells such as macrophages, B cells, monocytes and  
57 dendritic cells. They are highly polymorphic with multiple loci and alleles and this polymorphism  
58 gives the possibility to bind a large number of peptide ligands. Crystal structures of different MHC  
59 II proteins in mammals have shown that bound peptides are deeply integrated into the MHC  
60 structure using two main classes of interactions: 1) conserved hydrogen bonds to the peptide  
61 backbone; 2) at least four prominent pockets that accept peptide side chains [5-7].

62 In teleosts, MHC class I and II genes have been identified in various species and it has been  
63 established that class I and II loci **reside in different linkage groups** [8]. Fish MHC class II  
64 molecules are comprised of  $\alpha$  and  $\beta$  subunits, like in mammals, and **class II B loci are in separate**  
65 **linkage groups in all Euteleostei** [9]. MHC class II genes have been isolated from numerous fish  
66 species such as striped sea bass (*Morone saxatilis*) [10], red sea bream (*Chrysophrys major*) [11],  
67 various cichlids [12], salmonids [13-15] and different cyprinids [16-20].

68 MHC II genes in teleosts are also polymorphic and various studies have tried to establish the  
69 association of the MHC diversity [21-22] or differential gene expression [22-27] with disease  
70 resistance to virus and bacteria, as such associations were identified in humans [28] and chicken  
71 [29].

72 In this study we report the cloning and sequencing of the MHC class II  $\beta$  chain from sea bass  
73 (*Dicentrarchus labrax* L.), one of the most important species in aquaculture in the South  
74 Mediterranean, and studied **its basal expression levels** and under different “in vitro” conditions by

75 real-time PCR. These results will add a new tool for studying the effects of vaccination and  
76 immuno-stimulation on the sea bass immune system. Moreover, we predicted, for the first time, the  
77 3D structure of a MHC class II  $\beta$  chain from a teleost fish by homology modelling, a starting point  
78 for successive structural-functional investigations on this fundamental immune molecule.

79

80

81

82

83

84

85

86

87

88

89

90

91

92

93

94

95

96

97

98

99

100

101

102

103

104

105

106

107

108

109

110

111

112

113

114

115

## 2. MATERIALS AND METHODS

116

### 117 *2.1 Sea bass MHC class II $\beta$ chain cloning and sequencing*

118 Two degenerate primers (MHCFR1 5'- TGCWGYGYRTAYGRSTTCTACCC – 3' and  
119 MHCRV1 5' AGGCTKGKRTGCTCCACCWRRCA –3' where Y = C/T, K = G/T, R = G/A, S =  
120 G/C, W = A/T) corresponding to highly conserved regions of known MHC class II  $\beta$  genes [30]  
121 were used for RT-PCR on total RNA extracted with Tripure (Roche) solution from one juvenile sea  
122 bass (150 g of weight) head kidney. The leukocyte head kidney cells were obtained after Percoll  
123 purification as a single fraction following the procedures described in [31]. RT-PCR was performed  
124 using Ready-To-Go RT-PCR Beads (Amersham Pharmacia). For cDNA synthesis, 1  $\mu$ g of total  
125 RNA and 0.5  $\mu$ g of random primers [pd(N)<sub>6</sub>] were used in each reverse transcription reaction in a  
126 total volume of 50  $\mu$ l. Reactions were conducted using the Mastercycler personal (Eppendorf). The  
127 cycling protocol was one cycle of 94°C for 5 min, 35 cycles of 94°C for 45 s, 60°C for 45 s, 72°C  
128 for 45 s, followed by one cycle of 72 °C for 10 min. PCR products (15  $\mu$ l) were visualised on 1%  
129 (w/v) agarose gels containing ethidium bromide (10 ng/ml) using hyperladder IV (Bioline) as size  
130 marker. Controls for the presence of DNA contamination were performed using the RNA samples  
131 as template. DNA amplified by PCR was purified using the QIAquick Gel Extraction Kit (QIAGEN),  
132 inserted into the pGEM-T Easy vector (Promega) and transfected into competent JM109  
133 *Escherichia coli* cells. Plasmid DNA from at least ten independent clones was purified using the  
134 Wizard Plus SV Minipreps DNA Purification System (Promega) and sequenced using MWG DNA  
135 Sequencing Services. Sequences generated were analysed for similarity with other known MHC  
136 class II  $\beta$  sequences using the FASTA [32] and BLAST [33] programs and multiple alignments  
137 were made with MEGA 3.1 Software [34].

138 Further primers were designed based on the initial sea bass MHC class II  $\beta$  sequences for 5'-  
139 and 3'- rapid amplification of cDNA ends (RACE)-PCR (MHC-F1 5'-  
140 TCAGAGTGAGCTGGCTCAGA-3' and MHC-F2 5'-GGTCTGGAGAGAAGATCTCC-3'; MHC-

141 R1 5'-GGAACCAGAATCCTTCCTCG-3' and MHC-R2 5'- TGTGTTTGGGGTAGAAGCCG-  
142 3'). cDNA was synthesised from the same total head kidney RNA with the First-strand cDNA  
143 Synthesis kit (Amersham Pharmacia) following the manufacturers instructions. For 3' RACE-PCR,  
144 cDNA was transcribed from the same total head kidney RNA using an oligo-dT adaptor primer (5'-  
145 CTCGAGATCGATGCGGCCGCT<sub>15</sub>-3'). PCR was performed initially with the MHC-F1 primer  
146 and the oligo-dT adaptor primer, followed by a semi-nested PCR using MHC-F2 primer and the  
147 adaptor primer (5'-CTCGAGATCGATGCGGCCGC-3'). For 5' RACE-PCR, cDNA was  
148 transcribed from total RNA using the oligo-dT primer, treated with *E. coli* RNase H (Promega),  
149 purified using a PCR Purification Kit (QIAGEN), and tailed with poly(C) at the 5' end with terminal  
150 deoxynucleotidyl transferase (TdT, Promega). PCR was performed initially with MHC-R1 primer  
151 and an Oligo-dG primer (5'-GGGGGGIIGGGIIGGGIIG-3'), and then semi-nested with MHC-R2  
152 and the oligo-dG primers. Sequencing and similarity searches were as described above.

153 The obtained cDNA sequences were analysed for the presence of a signal peptide, using SignalP  
154 software [35], and of N- (with the NetNGlyc 1.0 Server) and O-linked glycosylation sites [36].  
155 Comparison of the sea bass MHC class II  $\beta$  amino acid sequences to their counterparts from other  
156 fish and mammalian species was carried out using the DIALIGN program [37]. A phylogenetic tree  
157 was constructed by the "neighbour-joining" method using MEGA 3.1 Software [34] on full-length  
158 amino acid sequences and bootstrap values calculated.

## 159 ***2.2 Basal MHC class II $\beta$ chain expression***

160 **To study the IL-10 basal expression, 5 sea bass juveniles (150 g of weight) were sampled**  
161 **and leucocytes from different tissues and organs [spleen, peripheral blood leukocytes (PBL),**  
162 **brain, liver, gut, thymus, head kidney (HK), gills] obtained as described in [31].**

163 **Total RNA was extracted with Tripure (Roche). For the reverse transcription the**  
164 **BioScript RNase H minus (Bioline) enzyme was used with the following protocol: 2  $\mu$ g of total**  
165 **RNA was mixed with 1  $\mu$ l of random hexamer (0.2  $\mu$ g/ $\mu$ l; Amersham Pharmacia) and nuclease**  
166 **free water was added to a final volume of 12  $\mu$ l. This mixture was incubated at 70° C for 5**

167 min and then cooled on ice. Successively, 0.4  $\mu$ l of a reaction mix containing 100 mM dNTPs  
168 (25mM each; Promega), 4 $\mu$ l of 5X Reaction buffer , nuclease free water to a final volume of  
169 19.75  $\mu$ l and 0.25  $\mu$ l of BioScript at 200 u/ $\mu$ l were added and the solution incubated first at 25  
170  $^{\circ}$ C for 10 min and than at 37  $^{\circ}$ C for 60 min. Finally, the reaction was stopped by heating at 70  
171  $^{\circ}$ C for 10 min.

172 The expression level of MHC class II  $\beta$  chain was determined with a Mx3000P<sup>TM</sup> real time  
173 PCR system (Stratagene) equipped with version 2.02 software and using the Brilliant SYBR  
174 Green Q-PCR Master Mix (Stratagene) following manufacturer's instructions, with ROX as  
175 internal reference dye. Specific PCR primers were designed for the amplification of about 200  
176 bp products from both MHC class II  $\beta$  chain and  $\beta$ -actin (used as housekeeping gene)  
177 transcripts. The primers were: RTMHCFR 5'-CAGAGACGGACAGGAAG-3' and  
178 RTMHCRV2 5'- CAAGATCAGACCCAGGA-3', RTACTFR2: 5'-  
179 ATGTACGTTGCCATCC-3' and RTACTRV2: 5'-GAGATGCCACGCTCTC-3',  
180 respectively. Approximately 50 ng of cDNA template was used in each PCR reaction. The  
181 PCR cycle conditions were 95  $^{\circ}$ C for 10 min, followed by 35 cycles of 95  $^{\circ}$ C for 45 s, 52  $^{\circ}$ C for  
182 45 s and 72  $^{\circ}$ C for 45 s. Triplicate reactions were performed for each template cDNA and the  
183 template was replaced with water in all blank control reactions. Each run was terminated  
184 with a melting curve analysis (all points method) which resulted in a melting peak profile  
185 specific for the amplified target DNA and the PCR products were examined by agarose gel  
186 electrophoresis. Fluorescence data were collected during the extension stage of amplification.  
187 Analysis of the data was carried out using the endpoints method option of the Mx3000P<sup>TM</sup>  
188 software.

189 Data were expressed as the mean  $\pm$  SE and the tissue with the lowest MHC class II  $\beta$   
190 chain expression was used as calibrator and the  $\beta$ -actin as the normaliser.

191 *2.3 In vitro sea bass MHC class II  $\beta$  chain expression after stimulation*

192 The “in vitro” expression of MHC class II  $\beta$  chain was studied by stimulating leukocytes  
193 isolated by Percoll gradients [31] from the head kidney of 5 sea bass juveniles (150 g of weight).

194 In one stimulation, the head kidney leucocytes from the single fishes after Percoll purification,  
195 were adjusted to  $1 \times 10^5$  cells/ml and incubated at 18 °C for 4 h and 24 h with 5  $\mu$ g/ml of  
196 lipopolysaccharide (LPS from *E. coli* 0127:B8, Sigma).

197 In another stimulation, the head kidney leucocytes from the single fishes after Percoll  
198 purification, were adjusted to  $1 \times 10^5$  cells/ml and incubated at 18 °C for 24 h in the presence of 10,  
199 30, 50 or 100 ng/ml of sea bass recombinant IL-1 $\beta$  (rIL-1 $\beta$ ) [38-39], with 50 ng/ml of rIL-1 $\beta$  heated  
200 at 95 °C for 20 min or with no recombinant protein, in 5 ml of L15 medium (Gibco).

201 Total RNA was extracted from experimental cultures after the stimulations with Tripure  
202 (Roche) and real-time PCR conditions were as described above for the basal expression.

203 Data were expressed as the mean  $\pm$  SE and the differences from the control at the same time  
204 have been considered significant if  $p < 0.05$  using the standard student *t* test to analyse the  
205 **significance**.

#### 206 ***2.4 Sea bass MHC class II $\beta$ chain protein modelling***

207 Three-dimensional models of sea bass MHC class II  $\beta$  chain were created following the  
208 homology modelling procedure described in previous papers [40-44], also in agreement with the  
209 rules recently reviewed [45] to improve the quality of the modelling results. The BLAST program  
210 [33] was used to find homologous proteins in databases. Structure predictions of sea bass MHC  
211 class II  $\beta$  chain were based on the availability of the three-dimensional models of the homologous  
212 mouse MHC I-A<sup>K</sup> chain  $\beta$  protein complexed with antigen peptide and D10 T-cell antigen receptor  
213 [46] (PDB code: 1D9K) and with antigen peptide and human CD4 [47] (PDB code: 1JL4). The  
214 alignment of the protein sequences was made with CLUSTALW program [48] and a few manual  
215 refinements were added to account for the position of secondary structures. Full-atom models of sea  
216 bass MHC were created with the MODELLER module [49] of Quanta (Accelrys, Inc., San Diego,

217 CA, USA) by using as template each of two crystallographic structures, by setting 4.0 Angstroms as  
218 RMS deviation among initial models and by full optimization of models, i.e. multiple cycles of  
219 refining with conjugate gradients minimization and molecular dynamics with simulated annealing.  
220 The best models were chosen by evaluating their stereochemical quality with the PROCHECK  
221 program [50] and a scoring function with ProsaII program [51]. Secondary structures were assigned  
222 by the DSSP program [52]. Search for structural classification was performed on CATH database  
223 [53]. The “Protein-Protein Interaction Server” (<http://www.biochem.ucl.ac.uk/bsm/PP/server>) [54]  
224 and the program NACCESS [55] were used to identify the amino acids at the protein-protein  
225 interface in the crystallographic complexes. Molecular superimposition, RMSD values and figures  
226 were obtained with the InsightII package (Accelrys, Inc., San Diego, CA, USA).

227  
228  
229  
230  
231  
232  
233  
234  
235  
236  
237  
238  
239  
240  
241  
242  
243  
244  
245  
246  
247  
248  
249  
250  
251  
252  
253  
254  
255  
256  
257

### 3. RESULTS

258

#### 3.1 Sea bass MHC class II $\beta$ chain cloning and sequencing

259

260 PCR with primers MHCFR1 and MHCRV1 resulted in products of the expected size (190 bp)  
261 with similarity to other known MHC class II  $\beta$  sequences (data not shown). 3'-RACE-PCR  
262 performed with MHC-F2 (based on the initial 190 bp sequence) and the adaptor primer to extend  
263 the sea bass MHC sequence gave a product of about 690 bp that contained the 3'-end of the gene.  
264 5'-RACE-PCR was then performed with MHC-R2 (based on the initial 190 bp sequence) and oligo-  
265 dG, and gave a product of about 460 bp that contained the 5'-end of the gene, with some differences  
266 between the selected clones. The six full-length nucleotide sequences (EMBL accession numbers  
267 AM113466, AM113467, AM113468, AM113469, AM113470, AM113471) are comprised of 1259  
268 and have been designated as Dila-DAB sequences (from \*0101 to \*0601). **They encode** for 250  
269 amino acids, with a predicted 21 amino acid signal peptide, and a 28 bp 5'-UTR and a 478 bp 3'-  
270 UTR (Fig. 1). The 3'-UTR contained a polyadenylation signal (AATAAA) 12 bp upstream of the  
271 poly(A) tail.

272 In order to verify the number of class II *B* loci, PCR of the open reading frame was performed  
273 on the cDNA used for the MHC class II  $\beta$  chain cloning with specific primers (MHCTOTFR 5'-  
274 GGCTTCATCCTTTCTCAG-3' and MHCTOTRV 5'-TACTGGGAACCAGAATCC-3') and 10  
275 clones were sequenced, confirming the presence of the six different sequences already obtained  
276 with the superimposition of the fragments coming from 3' and 5' RACE. In addition, 10 clones of  
277 the 3' UTR sequences from the same individual were sequenced and three different sequences were  
278 identified, which should demonstrate that sea bass seems to express **at least three class II *B* loci**.

279 A multiple alignment of the predicted translation of Dila-DAB sequences was assembled (Fig.  
280 1) together with some fish, mammalian and avian species to investigate the conservation of  
281 characteristic amino acid residues. The  $\beta$ -1 domain comprises of 92 amino acids, starts with an  
282 alanine residue, which is conserved in all fish sequences except in salmon (*Salmo salar*) and trout  
283 (*Oncorhynchus mykiss*), and contains few conserved amino acids (**11% identity** between fish

284 species). The  $\beta$ -2 domain is 94 amino acids long, starts with a valine residue conserved in all  
285 sequences except in Japanese flounder (*Paralichthys olivaceus*), red sea bream (*Pagrus major*) and  
286 cichlid (*Cyphotilapia frontosa*), shows high identity (35 %) in the C-proximal region and ends with  
287 a conserved tryptophan residue. The connecting peptide consists of 10 amino acids and the  
288 transmembrane domain, that contains 22 residues, and has the highest identity percentage (55 %).  
289 The cytoplasmic tail varies in length in the different species and starts with a conserved tyrosine  
290 residue in fish species. The cytoplasmic region contains 13 residues in the Dila-DAB sequences.

291 The cysteine residues present in the  $\beta$ -1 and  $\beta$ -2 domains are well conserved in all sequences  
292 except in the turbot sequence that lacks the cysteine at position 94 of the Dila-DAB sequences.  
293 These residues, presumably forming two disulfide intra-chain bonds, are consistent with previous  
294 findings in other species [56-57]. No potential O- or N-glycosylation sites were found in the Dila-  
295 DAB sequences, in contrast to one present in the red sea bream [11], in the catfish [58] and in  
296 rainbow trout [59-60].

297 Phylogenetic analysis (Fig. 2) conducted using amino acid sequences showed that all fish  
298 sequences are in the same cluster and that the six Dila-DAB sequences are in two different groups:  
299 one with sequences Dila-DAB\*0101, \*0201 and \*0301 and the other with sequences Dila-  
300 DAB\*0401, \*0501, \*0601. The first group of sea bass sequences also contains the striped bass  
301 Mosa-DAB sequence. The mammalian and avian sequences are in a different cluster with respect to  
302 the fish one.

### 303 **3.2 Basal MHC class II $\beta$ chain expression**

304 **The expression analysis of IL-10 in organs and tissues of unstimulated sea bass is shown in**  
305 **Figure 3. Real-time PCR products were loaded on agarose gels to exclude the formation of**  
306 **non-specific amplicons and, to take into consideration the individual genetic variability, five**  
307 **different fishes were sampled. MHC class II  $\beta$  chain levels were expressed as a ratio relative to**  
308  **$\beta$ -actin levels in the same samples after real-time PCR analysis using the tissue with the lowest**  
309 **expression as calibrator. The highest MHC class II  $\beta$  chain expression was detected in gills,**

310 followed by gut and thymus. Lower IL-10 mRNA levels were observed in spleen, PBL, and  
311 liver; brain and HK showed the lowest expression levels.

### 312 *3.3 In vitro sea bass MHC class II $\beta$ chain expression after stimulation*

313 To investigate the differential “in vitro” sea bass MHC class II  $\beta$  chain expression after  
314 stimulation with LPS at 4 and 24 hours and with various rIL-1 $\beta$  concentrations, we used RNA  
315 extracted from head kidney leucocytes. Total RNA from 5 different fishes was collected and real-  
316 time PCR primers were selected in the conserved region of all Dila-DAB sequences. After  
317 amplification and real-time analysis, PCR products for both MHC class II  $\beta$  and  $\beta$ -actin were  
318 loaded on agarose gels to exclude the formation of non-specific amplicons. Dila-DAB mRNA levels  
319 were compared to the housekeeping gene  $\beta$ -actin levels in the same samples and the values of the  
320 quantitative analysis were expressed as a ratio relative to  $\beta$ -actin.

321 Stimulation with LPS (Fig. 4A) resulted in very little differences in the MHC class II  $\beta$   
322 expression after 4 h with respect to the control at the same time and the statistical analysis  
323 performed showed that it was not significant. After 24 h the MHC expression has decreased to a  
324 large extent and, in this case, the difference was statistically significant. **Moreover, IL-1 $\beta$**   
325 **expression (data not shown) was studied in the same samples to be sure of the LPS stimulation**  
326 **and showed an increase of IL-1 $\beta$  levels, as was expected.**

327 Stimulation with different concentrations of rIL-1 $\beta$  (from 0 to 100 ng/ml) resulted in a dose-  
328 dependent reduction of the Dila-DAB expression (Fig. 4B), with the lowest value obtained from the  
329 sample treated with 100 ng/ml of rIL-1 $\beta$ . The differences were statistically significant for all the  
330 samples, except for the cell culture stimulated with 10 ng of rIL-1 $\beta$  and the cell culture stimulated  
331 with 50 ng/ml of rIL-1 $\beta$  pre-heated at 95 °C for 20 min. The latter observation is consistent with  
332 those reported by Hong et al., (2001) [61]. The Dila-DAB mRNA level in this case was almost  
333 equal to the control and significantly different with the sample stimulated with the same dose of  
334 rIL-1 $\beta$  but not heated.

### 335 *3.4 Sea bass MHC class II $\beta$ protein modelling*

336 The Dila-DAB sequences have been analysed with the BLAST program in order to find similar  
337 sequences in databases and to perform the structural predictions. The crystallographic structures of  
338 mouse MHC I-AK  $\beta$  chain complexed with D10 T-cell antigen receptor (PDB code: 1D9K) and  
339 human CD4 (PDB code: 1JL4) were selected as template models and the mouse sequence showed  
340 the maximum identity percentage (34%) with the Dila-DAB\*0101 sequence (data not shown). **This**  
341 **low level of sequence identity required an accurate procedure to build a 3D model of the**  
342 **protein by comparative modeling, in agreement with rules recently reviewed [45], as already**  
343 **applied in previous papers [40-44].**

344 We aligned the Dila-DAB\*0101 and mouse MHC sequences using the CLUSTALW program  
345 and we performed a few manual adjustments in order to remove gaps within  $\alpha$ -helices or  $\beta$ -strands  
346 (Figure 5). Starting from this alignment two sets of ten structural models were created, in two  
347 distinct sessions, for the Dila-DAB 17-206 region using the templates above indicated. We selected  
348 the best model created in each session, i.e. Model-<sup>1D9K</sup> and Model-<sup>1JL4</sup> by evaluating the stereo  
349 chemical quality of the models with the PROCHECK package [50] and a scoring function with  
350 ProsaII program [51]. The models have been deposited in the Protein Data Bank and accepted with  
351 the PDB codes 2H37 and 2H38, respectively.

352 Figure 6 shows the two Dila-DAB homology models with their secondary structure elements.  
353 These models have a classical organization in two distinct domains in agreement with the structural  
354 classification reported by CATH database [53] for the model structures of mouse MHC class II  $\beta$   
355 chain. The N-terminal domains are classified as “alpha-beta” and consist of an alpha helical region  
356 and a beta sheet of four strands in antiparallel orientation. The C-terminal domains have a “mainly  
357 beta” fold and are characterized by an immunoglobulin-like beta-sandwich made of two antiparallel  
358 sheets, each consisting of three main strands and few shorter strands, organized in greek-keys  
359 motifs. In both models of Dila-DAB four cysteine residues are located in the same positions of the  
360 mouse structures and they may form an S-S bond (30-95) in the N-terminal domains, and another S-

361 S bond (133-189) in the C-terminal domains between the two sheets of the sandwich architecture, as  
362 described in mammals [56-57].

363 The two Dila-DAB models were compared by structural superimposition, RMSD evaluation and  
364 secondary structures (Figure 5) to evidence structural changes due to the binding with different  
365 ligands (in one case T-cell receptor and in another CD4). The presence of gaps in the alignment  
366 made it difficult to perform a complete structural comparison of Dila-DAB models with the  
367 template structures. Superimposition of structurally conserved regions of Dila-DAB Model-<sup>1JL4</sup> and  
368 Model-<sup>1D9K</sup> with their respective templates gave RMSD values of 1 Angstrom and 0.96 Angstrom,  
369 respectively. In contrast, an RMSD value of 1.22 Angstrom was obtained by superimposition of the  
370 two Dila-DAB models, i.e. Model-<sup>1D9K</sup> and Model-<sup>1JL4</sup>, indicating that these two conformations  
371 present some structural differences.

372 The comparison of secondary structures, assigned by DSSP program in all four models, shows  
373 that the alpha helices and the beta-strands are quite conserved in the mouse and Dila-DAB models,  
374 although some differences are noted. The short  $3_{10}$  helix (GTQ) observed in both crystallographic  
375 mouse structures is not present in the two Dila-DAB models. In Dila-DAB Model-<sup>1JL4</sup> an alpha helix  
376 (Tyr<sup>103</sup>-Lys<sup>110</sup>) is observed where in mouse MHC I-A<sup>K</sup> complexed with human CD4 (PDB code:  
377 1JL4) a short  $3_{10}$  helix (SLR) is present. By comparing the two Dila-DAB models, we note that  
378 Model-<sup>1D9K</sup> has a lower content of beta-strand in the C-terminal domain, where the strands include  
379 **fewer** amino acids and are often broken in two shorter strands. In particular, two short beta-strands,  
380 spanning residues Tyr<sup>171</sup>-Ile<sup>173</sup> and His<sup>176</sup>-Tyr<sup>179</sup>, are present in Model-<sup>1D9K</sup>, while only one long  
381 beta-strand (Tyr<sup>171</sup>-Tyr<sup>179</sup>) is present in Model-<sup>1JL4</sup>. Moreover, Model-<sup>1JL4</sup> shows one more short  
382 beta strand (Val<sup>158</sup>-Ser<sup>160</sup>), similar to its template.

383 Finally, we analyzed the mouse structures to identify the regions involved in the interactions  
384 with peptides, T-cell antigen receptor and CD4, by means of solvent accessibility and protein-  
385 protein interaction analyses (data not shown). By homology considerations, the aligned regions in  
386 the Dila-DAB sequence can be hypothesized to be similarly involved in ligand binding.

387  
388  
389  
390  
391  
392  
393  
394  
395  
396  
397  
398  
399  
400  
401  
402  
403  
404  
405  
406  
407  
408  
409  
410  
411  
412  
413  
414  
415  
416  
417  
418  
419  
420  
421  
422  
423  
424  
425  
426  
427  
428  
429  
430  
431  
432  
433  
434

#### **4. DISCUSSION**

435 The MHC class I and class II molecules are involved in the presentation of antigens to the  
436 adaptive immune system. High polymorphism in MHC molecules has been observed in vertebrates  
437 and growing **evidence suggests** that MHC variants influence many important biological traits,  
438 including immune recognition, susceptibility to infectious and autoimmune diseases, mating  
439 preferences and pregnancy outcome [62]. For these reasons MHC genes are among the best  
440 candidates for studies of mechanisms and significance of molecular adaptation in vertebrates.

441 In this study, we report the homology cloning of the MHC class II  $\beta$  chain from the teleost sea  
442 bass (*Dicentrarchus labrax*). Six different sequences, named Dila-DAB, were obtained. The Dila-  
443 DAB cDNAs were predicted to code for proteins of 250 amino acids and their size was in  
444 accordance with other fish and mammalian MHC class II  $\beta$  chain molecules. The alignment of  
445 Figure 1 showed that the  $\beta$ -1 domains present a **variability** indicative of a functional peptide  
446 binding region and most of the differences between the six Dila-DAB sequences are in this region.  
447 On the contrary, the  $\beta$ -2 domains are quite well conserved, especially in the membrane-proximal  
448 region. Proposed sites for the interaction of the MHC class II  $\beta$  chain with the MHC class II  $\alpha$  chain  
449 in mammals [57-58] involve three amino acid residues: two histidines and a glutamic acid. Two of  
450 these residues are conserved in all fish sequences (His<sup>127</sup> and Glu<sup>178</sup> in the Dila-DAB sequences),  
451 while the second histidine residue is substituted in the majority of fish molecules by a proline  
452 (Pro<sup>128</sup> in the Dila-DAB sequences). Putative sites important for human MHC class II  $\beta$  chain  
453 interaction with CD4 co-receptor are three residues: a valine, a threonine and a serine [57], and  
454 these residues are conserved in all fish sequences (Val<sup>158</sup>, Thr<sup>159</sup>, Ser<sup>160</sup> in the Dila-DAB  
455 sequences). The transmembrane domain is highly conserved and has multiple hydrophobic residues  
456 that are interspersed with uncharged glycines at position 219, 222, 226 and 233 in the Dila-DAB  
457 sequences as seen in the sequences from other species [63].

458 Phylogenetic analysis, generated using amino acid sequences, showed a close relationship  
459 between the Dila-DAB and Mosa-DAB sequences (Fig. 2) providing evidence for trans-species

460 evolution of the class II sequences. The bootstrapped tree was divided into two different branches  
461 with one containing all fish sequences and the other with mammalian and avian ones.

462 **Moreover, our data suggest that MHC class II  $\beta$  is present in a ubiquitous manner in non-**  
463 **stimulated tissues and organs, although with different expression levels. The highest**  
464 **expression was found in gills that in fish are constantly exposed to a plethora of water born**  
465 **antigens. Moreover, some pathogens use the gills as a portal of entry into the host [64] while**  
466 **others use this organ as the site of infection [65]. Therefore, the ability to mount strong local**  
467 **immune reactions to pathogens is fundamental to avoid disease as already observed in**  
468 **Atlantic salmon [66]. It should be noted that expression of MHC class II  $\beta$  is notably elevated**  
469 **in the gut that is a mucosal tissue particularly rich in T-cells in sea bass [67].**

470 The “in vitro” MHC class II  $\beta$  chain expression was studied using head kidney leukocytes, because  
471 this tissue in the red sea bream, a species related to sea bass, showed the highest basal MHC  $\beta$  chain  
472 expression [11]. The selected stimulants were LPS, to simulate a pathogen infection, and the sea  
473 bass rIL-1 $\beta$ . This cytokine was chosen as it should promote phagocytosis of foreign particles, which  
474 are subsequently presented to T-cells in conjunction with MHC molecules [68]. LPS stimulation  
475 resulted in a down-regulation of Dila-DAB, which was statistically significant after 24 h and in an  
476 increase of IL-1 $\beta$  gene expression (data not shown), that was used to test the efficacy of the  
477 activation. This is in accordance with the results found in a macrophage-like cell line (SHK-1)  
478 derived from Atlantic salmon [69-70]. **A similar down-regulation of MHC class II was also**  
479 **obtained after challenge with *Vibrio anguillarum* in red sea bream [11] and of MHC class I**  
480 **after infection with hematopoietic necrosis virus (IHNV) in rainbow trout [71].** Recombinant  
481 sea bass IL-1 $\beta$  produced a dose-dependent down-regulation in the concentrations used and this has  
482 also been observed in various human cell types [72]. It has been postulated that IL-1 $\beta$  plays a role  
483 in regulating immunoreactivity by inhibiting transcription of the CIITA gene, thereby reducing  
484 class II MHC expression in mammal cell lines [73]. The stimulation has also been performed with

485 heat inactivated rIL-1 $\beta$  to confirm that the observed down-regulation was due to the cytokine  
486 stimulation. **MHC down-regulation could be very likely linked to the already reported**  
487 **mechanisms for the control of inflammation responses in mammals that, uncontrolled, may**  
488 **have dangerous effects. During early inflammation, various cytokines are produced and they**  
489 **down-regulate the expression of inflammation-related molecules [74]. More experiments and**  
490 **tools will be required to demonstrate that something similar happens in fish.**

491 The **percentage identity** between the N-terminal region of the Dila-DAB\*0101 sequence  
492 (amino acids 17-206) and mouse MHC sequence, for which crystallographic structures complexed  
493 with D10 T-cell antigen receptor and human CD4 are available, gave us the opportunity to apply  
494 homology modelling techniques and study the predicted 3D Dila-DAB structures. The two obtained  
495 models (Fig. 5) differ mainly in the ligand binding regions. In Model-<sup>1JL4</sup>, we observed that both  
496 the antigen peptide binding site (1360 vs 1309 Angstrom<sup>2</sup>) and the interaction surface with CD4  
497 (775 vs 742 Angstrom<sup>2</sup>) were larger than in the Model-<sup>1D9K</sup>. On the contrary, the interaction surface  
498 with the T-cell antigen receptor was larger in Model-<sup>1D9K</sup> (1144 vs 1095 Angstrom<sup>2</sup>). **The fact that**  
499 **each model presents a larger interaction surface for the respective ligand confirms the**  
500 **reliability of the prediction. The experimental use of synthetic peptides designed on the basis**  
501 **of the amino acids present on the interaction surfaces with the two different ligands should**  
502 **block the non-covalent bond and will be useful to confirm the structural prediction and for**  
503 **functional investigations.**

504 **In conclusion, the availability of these Dila-DAB sequences will add new insight into the**  
505 **MHC variability in vertebrates, that is linked to parasite resistance, and will give the**  
506 **possibility to analyse the sea bass MHC class II expression levels after vaccination and**  
507 **immuno-stimulation protocols.**

## 508 REFERENCES

509 [1] Auffray C, Strominger JL. Molecular genetics of the human major histocompatibility complex.  
510 Adv Hum Genet 1986; 15:197-247.

- 511 [2] Lanzavecchia A. Receptor mediated antigen uptake and its effect on antigen presentation to  
512 class II-restricted T lymphocytes. *Ann Rev Immunol* 1990; 8:773-93.
- 513 [3] Konig R, Huang L-Y, Germain RN. MHC class II interaction with CD4 mediated by a region  
514 analogous to the MHC class binding site. *Nature* 1992; 356:796-98.
- 515 [4] Brodsky FM, Guagliardi LE. The cell biology of antigen processing and presentation. *Ann Rev*  
516 *Immunol* 1991; 9:707-44.
- 517 [5] Fremont DH, Monnaie D, Nelson CA, Hendrickson WA, Unanue ER. Crystal structure of I-A<sup>k</sup>  
518 in complex with a dominant epitope of lysozyme. *Immunity* 1998; 8:305-17.
- 519 [6] Scott CA, Peterson PA, Teyton L, Wilson IA. Crystal structures of two I-A<sup>d</sup>-peptide complexes  
520 reveal that high affinity can be achieved without large anchor residues. *Immunity* 1998; 8:319-  
521 29.
- 522 [7] McFarland BJ, Katz JF, Sant AJ, Beeson C. Energetics and cooperativity of the hydrogen  
523 bonding and anchor interactions that bind peptides to MHC class II protein. *J Mol Biol* 2005;  
524 350: 170-83.
- 525 [8] Stet RJM, Kruiswijk CP, Dixon B. Major histocompatibility lineages and immune gene function  
526 in teleost fishes: the road not taken. *Crit Rev Immunol* 2003; 23:441-71.
- 527 [9] Sato A, Figueroa F, Murray BW, Malaga-Trillo E, Zaleska-Rutczynska Z, Sultmann H et al.  
528 Nonlinkage of major histocompatibility complex class I and class II loci in bony fishes.  
529 *Immunogenetics* 2000; 51:108-16.
- 530 [10] Walker RB, McConnell TJ, Walker RA. Variability in a MHC Mosa class II beta chain-  
531 encoding gene in striped bass (*Morone saxatilis*). *Dev Comp Immunol* 1994; 18:325-42.
- 532 [11] Chen S-L, Zhang Y-X, Xu M-Y, Ji X-S, Yu G-C, Dong C-F. Molecular polymorphism and  
533 expression analysis of MHC class II *B* gene from red sea bream (*Chrysophrys major*). *Dev*  
534 *Comp Immunol* 2006; 30: 407-18.
- 535 [12] Figueroa F, Mayer WE, Sultmann H, O'hUigin C, Tichy H, Satta Y et al. MHC class II *B* gene  
536 evolution in East African cichlid fishes. *Immunogenetics* 2000; 51:556-75.

- 537 [13] Miller KM, Withler RE. Sequence analysis of a polymorphic *MHC* class II gene in Pacific  
538 salmon. *Immunogenetics* 1996; 43:337-51.
- 539 [14] Ristow SS, Grabowski LD, Thompson SM, Warr GW, Kaattari SL, de Avila JM, Thorgaard  
540 GH. Coding sequences of the MHC II  $\beta$  chain of homozygous rainbow trout (*Oncorhynchus*  
541 *mykiss*). *Dev Comp Immunol* 1999; 23:51-60.
- 542 [15] Stet RJM, de Vries B, Mudde K, Hermsen T, van Heerwaarden J, Shump BP, Grimholt U.  
543 Unique haplotypes of co-segregating major histocompatibility class II A and class II B alleles  
544 in Atlantic salmon (*Salmo salar*) give rise to diverse class II genotypes. *Immunogenetics*  
545 2002; 54:320-31.
- 546 [16] Sultmann H, Mayer WE, Figueroa F, O'hUigin C, Klein J. Zebrafish *MHC* class II  $\alpha$  chain-  
547 encoding genes: polymorphism, expression, and function. *Immunogenetics* 1993; 38: 408-20.
- 548 [17] Dixon B, Nagelkerke LAJ, Sibbing FA, Egberts E, Stet RJM. Evolution of *MHC* class II  $\beta$   
549 chain-encoding genes in the Lake Tana barbell species flock (*Barbus intermedius* complex).  
550 *Immunogenetics* 1996; 44: 419-31.
- 551 [18] Graser R, O'hUigin C, Vincek V, Meyer A, Klein J. Trans-species polymorphism of class II  
552 *MHC* loci in danio fishes. *Immunogenetics* 1996; 44:36-48.
- 553 [19] van Erp SHM, Egberts E, Stet RJM. Characterization of major histocompatibility complex  
554 class II A and B genes in a gynogenetic carp clone. *Immunogenetics* 1996; 44:192-202.
- 555 [20] Stet RJM, Kruiswijk CP, Saeij JPJ, Wiegertjes GF. Major histocompatibility genes in cyprinid  
556 fishes: theory and practice. *Immunological Reviews* 1998; 166:301-16.
- 557 [21] Grimholt U, Larsen S, Nordmo R, Midtlyng P, Kjoeglum S, Storset A, et al. *MHC*  
558 polymorphism and disease resistance in Atlantic salmon (*Salmo salar*); facing pathogens with  
559 single expressed major histocompatibility class I and class II loci. *Immunogenetics* 2003;  
560 55:210-19.

- 561 [22] Kurtz J, Kalbe M, Aeschlimann PB, Haberli MA, Wegner KM, Reusch TB, Milinski M. Major  
562 histocompatibility complex diversity influences parasite resistance and innate immunity in  
563 sticklebacks. *Proc Biol Sci* 2004; 271:197-204.
- 564 [23] Koppang EO, Lundin M, Press McL, Ronningen K, Lie O. Differing levels of Mhc class II  $\beta$   
565 chain expression in a range of tissues from vaccinated and non-vaccinated Atlantic salmon  
566 (*Salmo salar* L.). *Fish Shellfish Immunol* 1998; 8:183-96.
- 567 [24] Park KC, Osborne JA, Tsoi SC, Brown LL, Johnson SC. Expressed sequence tags analysis of  
568 Atlantic halibut (*Hippoglossus hippoglossus*) liver, kidney and spleen tissues following  
569 vaccination against *Vibrio anguillarum* and *Aeromonas salmonicida*. *Fish Shellfish Immunol*  
570 2005; 18:393-415.
- 571 [25] Tafalla C, Coll J, Secombes CJ. Expression of genes related to the early immune response in  
572 rainbow trout (*Oncorhynchus mykiss*) after viral haemorrhagic septicemia virus (VHSV)  
573 infection. *Dev Comp Immunol* 2005; 29:615-26.
- 574 [26] Morrison RN, Koppang EO, Hordvik I, Nowak BF. MHC class II<sup>(+)</sup> cells in the gills of Atlantic  
575 salmon (*Salmo salar* L.) affected by amoebic gill disease. *Vet Immunol Immunopathol* 2006;  
576 109:297-303.
- 577 [27] Wegner KM, Kalbe M, Rauch G, Kurtz J, Schaschl H, Reusch TB. Genetic variation in MHC  
578 class II expression and interactions with MHC sequence polymorphism in three-spined  
579 sticklebacks. *Mol Ecol* 2006; 15: 1153-64.
- 580 [28] Hill AV, Allsopp CEM, Kwiatkowski D, Anstey NM, Twumasi P, Rowe PA, et al. Common  
581 West African HLA antigens are associated with protection from severe malaria. *Nature* 1991;  
582 352:595-600.
- 583 [29] Hofmann A, Plachy J, Hunt L, Kaufman J, Hala K. v-src oncogene-specific carboxy-terminal  
584 peptide is immunoprotective against Rous sarcoma growth in chickens with MHC class I  
585 allele B-F12. *Vaccine* 2003; 21:4694-9.

- 586 [30] Venkatesh B, Ning Y, Brenner S. Late changes in spliceosomal introns define clades in  
587 vertebrate evolution. Proc Natl Acad Sci USA 1999; 96: 10267-71.
- 588 [31] Scapigliati G, Buonocore F, Bird S, Zou J, Pelegrin P, Falasca C, Prugnoli D, Secombes CJ.  
589 Phylogeny of cytokines: molecular cloning and expression analysis of sea bass *Dicentrarchus*  
590 *labrax* interleukin-1 beta. Fish Shellfish Immunol 2001; 11:711-26.
- 591 [32] Pearson WR, Lipman DJ. Improved tools for biological sequence comparison. Proc Natl Acad  
592 Sci USA 1988; 85:2444-8.
- 593 [33] Altschul SF, Gish W, Miller W, Myers E, Lipman DJ. Best local alignment search tool. J Mol  
594 Biol 1990; 215:403-10.
- 595 [34] Kumar S, Tamura K, Nei M (2004). MEGA3: Integrated Software for Molecular Evolutionary  
596 Genetics Analysis and Sequence Alignment. Briefings in Bioinformatics 2004; 5: 150-63.
- 597 [35] Nielsen H, Engelbrecht J, Brunak S, von Heijne G. Identification of prokaryotic and eukaryotic  
598 signal peptides and prediction of their cleavage sites. Protein Eng 1997; 10:1-6.
- 599 [36] Julenius K, Molgaard A, Gupta R, Brunak S. Prediction, conservation analysis and structural  
600 characterization of mammalian mucin-type O-glycosylation sites. Glycobiology 2005; 15:153-  
601 64.
- 602 [37] Brudno M, Chapman M, Gottgens B, Batzoglou S, Morgenstern B. Fast and sensitive multiple  
603 alignment of large genomic sequences. BMC Bioinformatics 2003; 4:66-77.
- 604 [38] Buonocore F, Mazzini M, Forlenza M, Randelli E, Secombes CJ, Zou J, Scapigliati G.  
605 Expression in *Escherichia coli* and purification of sea bass (*Dicentrarchus labrax*)  
606 interleukin-1 $\beta$ , a possible immuno-adjuvant in aquaculture. Marine Biotech. 2004; 6:53-9.
- 607 [39] Buonocore F, Forlenza M, Randelli E, Benedetti S, Bossù P, Meloni S, et al. Biological  
608 activity of sea bass (*Dicentrarchus labrax*) recombinant interleukin-1 $\beta$ . Marine Biotech. 2005;  
609 7:609-17.

- 610 [40] Facchiano AM, Stiuso P, Chiusano ML, Caraglia M, Giuberti G, Marra M, et al. Homology  
611 modelling of the human eukaryotic initiation factor 5A (eIF-5A). *Protein Engineering* 2001;  
612 14: 881-90.
- 613 [41] Marabotti A, D'Auria S, Rossi M, Facchiano AM. Theoretical model of the three-dimensional  
614 structure of a sugar binding protein from *Pyrococcus horikoshii*: structural analysis and sugar  
615 binding simulations. *Biochem J* 2004; 280:677-84.
- 616 [42] Scapigliati G, Costantini S, Colonna G, Facchiano A, Buonocore F, Bossù P, et al. Modelling  
617 of fish interleukin 1 and its receptor. *Dev Comp Immunol* 2004; 28:429-41.
- 618 [43] Costantini S, Colonna G, Rossi M, Facchiano AM. Modelling of HLA-DQ2 and simulations of  
619 its interaction with gluten peptides to explain molecular recognition in celiac disease. *J*  
620 *Molecular Graphics and Modelling* 2005; 23:419-31.
- 621 [44] Buonocore F, Randelli E, Bird S, Secombes CJ, Costantini S, Facchiano A, et al. The  
622 CD8alpha from sea bass (*Dicentrarchus labrax* L.): cloning, expression and 3D modelling.  
623 *Fish Shellfish Immunol* 2006; 20:637-46.
- 624 [45] Wallner B, Elofsson A. All are not equal: a benchmark of different homology modelling  
625 programs. *Protein Science* 2005; 14:1315-27.
- 626 [46] Reinherz EL, Tan K, Tang L, Kern P, Liu J, Xiong Y, et al. The crystal structure of a T cell  
627 receptor in complex with peptide and MHC class II. *Science* 1999; 286:1913-21.
- 628 [47] Wang JH, Meijers R, Xiong Y, Liu JH, Sakihama T, Zhang R, et al. Crystal structure of the  
629 human CD4 N-terminal two-domain fragment complexed to a class II MHC molecule. *Proc*  
630 *Natl Acad Sci USA* 2001; 98:10799-804.
- 631 [48] Thompson JD, Higgins DG, Gibson TJ. Clustal W: Improving the sensitivity of progressive  
632 multiple sequence alignment through sequence weighting, position-specific gap penalties and  
633 weight matrix choice. *Nucl Acids Res* 1994; 22:4673-80.
- 634 [49] Sali A, Blundell TL. Comparative protein modelling by satisfaction of spatial restraints. *J Mol*  
635 *Biol* 1993; 234:779-815.

- 636 [50] Laskowski RA, MacArthur MW, Moss DS, Thornton JM PROCHECK: a program to check the  
637 stereochemical quality of protein structures. *J Appl Cryst* 1993;26:283-91.
- 638 [51] Sippl MJ. Recognition of errors in three-dimensional structures of proteins. *Proteins* 1993;  
639 17:355-62.
- 640 [52] Kabsch W, Sander C. Dictionary of protein secondary structure: pattern recognition of  
641 hydrogen-bonded and geometrical features. *Biopolymers* 1983;22: 2577-637.
- 642 [53] Orengo CA, Michie AD, Jones S, Jones DT, Swindells MB, Thornton JM. CATH--a hierarchic  
643 classification of protein domain structures. *Structure* 1997;5:1093-108.
- 644 [54] Jones S, Thornton JM. Principles of protein-protein interactions derived from structural  
645 studies. *Proc Natl Acad Sci* 1996;93:13-20.
- 646 [55] Hubbard SJ, Campbell SF, Thornton JM. Molecular recognition. Conformational analysis of  
647 limited proteolytic sites and serine proteinase protein inhibitors. *J Mol Biol* 1991;220:507-30.
- 648 [56] Klein J. Natural history of the major histocompatibility complex. New York: John Wiley;  
649 1986.
- 650 [57] Brown JH, Jardetzky TS, Gorga JC, Stern LJ, Urban RG, Strominger JL, Wiley DC. Three-  
651 dimensional structure of the human class II histocompatibility antigen HLA-DR1. *Nature*  
652 1993; 364: 33-9.
- 653 [58] Godwin UB, Antao A, Wilson MR, Chinchar G, Miller NW, Clem W, McConnell TJ. MHC  
654 class II *B* genes in the channel catfish (*Ictalurus punctatus*). *Dev Comp Immunol* 1997;21:13-  
655 23.
- 656 [59] van Lierop M-J C, Knight J, Secombes CJ, Hermsen TT, Groeneveld A, Stet JM. Production  
657 and characterisation of an antiserum raised against recombinant rainbow trout (*Oncorhynchus*  
658 *mykiss*) MHC class II beta-chain (*MhcOnmy-DAB*). *Fish Shellfish Immunol* 1998;8:231-43.
- 659 [60] Nath S, Kales S, Fujiki K, Dixon B. Major histocompatibility class II genes in rainbow  
660 trout (*Oncorhynchus mykiss*) exhibit temperature dependent downregulation.  
661 ***Immunogenetics* 2006; 58: 443-53.**

- 662 [61] Hong S, Zou J, Crampe M, Peddie S, Scapigliati G, Bols N, et al. The production and  
663 bioactivity of rainbow trout (*Oncorhynchus mykiss*) recombinant IL-1 $\beta$ . *Vet Immunol*  
664 *Immunopatol* 2001;81:1-14.
- 665 [62] Sommer S. The importance of immune gene variability (MHC) in evolutionary ecology and  
666 conservation. *Front Zool* 2005; 2:16.
- 667 [63] Cosson P, Bonifacino JS. Role of the transmembrane domain interactions in the assembly of  
668 class II MHC molecules. *Science* 1992; 258:659-62.
- 669 [64] **Morris DJ, Adams A, Richards RH. In situ hybridisation identifies the gill as a portal of**  
670 **entry for PKK (Phylum Myxozoa), the causative agent of proliferative kidney disease in**  
671 **salmonids. *Parasitol. Res.* 2000; 86: 950-6.**
- 672 [65] **Ramsay E, Falk K, Mikalsen AB, Teig A. Xenoma formation during microsporidial gill**  
673 **disease of salmonids caused by *Loma salmonae* is affected by host species (*Oncorhynchus***  
674 ***tshawytscha*, *O. kisutch*, *O. mykiss*) but not by salinity. *Dis Aquat Org* 2002 ; 48: 125-31.**
- 675 [66] **Morrison RN, Koppang EO, Hordvik I., Nowak BF. MHC class II+ cells in the gills of the**  
676 **Atlantic salmon (*Salmo salar* L.) affected by amoebic gill disease. *Vet Immunol***  
677 ***Immunopatol* 2006; 297-303.**
- 678 [67] **Abelli L., Picchiatti S., Romano N., Mastrolia L., Scapigliati G. 1997.**  
679 **Immunohistochemistry of gut-associated lymphoid tissue of the sea bass *Dicentrarchus***  
680 ***labrax* (L.). *Fish Shellfish Immunol* 1997; 7: 235-46.**
- 681
- 682 [68] Dinarello CA. The interleukin-1 family: 10 years of discovery. *Fed Am Soc Exp Biol* 1994;  
683 8:1314-25.
- 684 [69] Koppang EO, Dannevig BH, Lie O, Ronningen K, Press CM. Expression of the MHC class I  
685 and II mRNA in a macrophage-like cell line (SHK-1) derived from Atlantic salmon, *Salmo*  
686 *salar*, head kidney. *Fish Shellfish Immunol* 1999; 9:473-89.

- 687 [70] Fast MD, Ross NW, Johnson SC. Prostaglandin E<sub>2</sub> modulation of gene expression in an  
688 Atlantic salmon (*Salmo salar*) macrophage-like cell line (SHK-1). Dev Comp Immunol 2005;  
689 29:951-63.
- 690 [71] Hansen JD, La Patra S. Induction of the rainbow trout MHC class I pathway during acute  
691 IHNV infection. Immunogenetics 2002;54:654-61.
- 692 [72] Watanabe Y, Lee S, Allison AC. Control of the expression of a class II major  
693 histocompatibility gene (HLA-DR) in various human cell types: down-regulation by IL-1 but  
694 not IL-6, prostaglandin E<sub>2</sub>, or glucocorticoids. Scand J Immunol 1990;32:601-9.
- 695 [73] Rohn W, Tang LP, Dong W, Benveniste ET. IL-1 $\beta$  inhibits IFN- $\gamma$ -induced class II MHC  
696 expression by suppressing transcription of the class II transactivator gene. J Immunol 1999;  
697 162:886-96.
- 698 [74] Coronel A, Boyer A, Franssen JD, Romet-Lemonne JL, Fridman WH, Teillaud JL.  
699 **Cytokine production and T-cell activation by macrophage-dendritic cells generated for**  
700 **therapeutic use. Br J Haematol 2001; 114: 671-80.**

#### 701 ACKNOWLEDGEMENTS

702 This work was supported by the European Commission within the project IMAQUANIM (EC  
703 contract number FOOD-CT-2005-007103).

704

705

706

707

708

#### FIGURE LEGENDS

709 **Fig. 1.** Alignment of the predicted sea bass Dila-DAB amino acid sequences with other known  
710 MHC class II  $\beta$  chain molecules. Regions corresponding to the putative signal peptide,  
711  $\beta$ -1 domain,  $\beta$ -2 domain, connecting peptide, transmembrane region and cytoplasmic tail  
712 are shown above the sequences. Conserved cysteine residues are evidenced in bold,

713 conserved amino acid residues are indicated with an asterisk, while amino acid residues  
714 present at the starting point of the different regions considering the human crystal  
715 structure are in bold and underlined. Accession numbers: Dila-DAB \*0101  
716 (*Dicentrarchus labrax*) AM113466; Dila-DAB \*0201 (*Dicentrarchus labrax*)  
717 AM113467; Dila-DAB \*0301 (*Dicentrarchus labrax*) AM113468; Dila-DAB \*0401  
718 (*Dicentrarchus labrax*) AM113469; Dila-DAB \*0501 (*Dicentrarchus labrax*)  
719 AM113470; Dila-DAB \*0601 (*Dicentrarchus labrax*) AM113471; Japanese flounder  
720 (*Paralichthys olivaceus*) AY848955; turbot (*Scophthalmus maximus*) DQ001730;  
721 Atlantic salmon (*Salmo salar*) X70167; red sea bream (*Pagrus major*) AY190711;  
722 striped sea bass (*Morone saxatilis*) L33967; rainbow trout (*Oncorhynchus mykiss*)  
723 AF115529; catfish (*Ictalurus punctatus*) U77597; humphead cichlid (*Cyphotilapia*  
724 *frontosa*) L13231; human (*Homo sapiens*) CAA47028; mouse (*Mus musculus*)  
725 AAC05286); chicken (*Gallus gallus*) NP\_001038144).

726 **Fig. 2.** Phylogenetic tree showing the relationship between Dila-DAB sequences with other  
727 known MHC class II  $\beta$  molecules. The tree was constructed by the “neighbour-joining”  
728 method and was bootstrapped 10000 times. 0.1 indicates the genetic distance.

729 **Fig. 3. MHC class II  $\beta$  chain basal expression in different tissues [spleen, peripheral blood**  
730 **leukocytes (PBL), brain, liver, gut, thymus, head kidney (HK), gills]. MHC class II**  
731  **$\beta$  mRNA levels were expressed as a ratio relative to  $\beta$ -actin levels in the same**  
732 **samples after real-time PCR analysis using the tissue with the lowest expression as**  
733 **calibrator.**

734 **Fig. 4.** MHC class II  $\beta$  expression in different stimulating conditions. (A): MHC mRNA levels  
735 expressed as a ratio relative to  $\beta$ -actin levels in the same samples after real-time PCR  
736 analysis of the head kidney leukocytes stimulated with no LPS (control) and with LPS  
737 for 4 and 24 h. (B): MHC mRNA levels expressed as a ratio relative to  $\beta$ -actin levels in

738 the same samples after real-time PCR analysis of the head kidney leukocytes stimulated  
739 with various rIL-1 $\beta$  concentrations.

740 Data were expressed as the mean  $\pm$  SE, \* indicates  $p < 0.05$  and therefore significantly  
741 lower than the respective control.

742 **Fig. 5.** Primary and secondary structures of mouse and Dila-DAB\*0101 chains, aligned as for  
743 the modelling procedure. Stars (\*) indicate identical amino acids. The interaction  
744 residues of mouse MHC-II with the antigen peptide, the D10 T-cell antigen receptors  
745 alpha and beta chains (N-terminal region) and human CD4 (C-terminal region) are  
746 reported in bold. Helices and beta strands are marked with continuous and dashed line  
747 boxes, respectively.

748 **Fig. 6.** Molecular models of sea bass MHC class II  $\beta$  obtained by homology modelling using as  
749 template the structure of mouse MHC I-A<sup>K</sup> chain  $\beta$  complexed with human CD4, i.e.  
750 Models-<sup>1JL4</sup> (a) and with D10 T-cell antigen receptor, i.e. Models-<sup>1D9K</sup> (b). Backbone  
751 ribbon and the secondary structure topology are shown: yellow arrows represent beta  
752 strands, red cylinders represent alpha helices. Amino and carboxy terminal ends are  
753 indicated. Green and yellow sticks indicate the possible presence of two Cys-Cys bonds  
754 in each model.

755  
756  
757